# Cryptophane-Xenon Complexes in Organic Solvents Observed through NMR Spectroscopy

**Gaspard Huber,[†] Lætitia Beguin,[†] Hervé Desvaux,[†] Thierry Brotin,[‡] Heather A. Fogarty,[‡] Jean-Pierre Dutasta,[‡] and Patrick Berthault*,[‡]**

*CEA, IRAMIS, Service de Chimie Moléculaire, Laboratoire Structure et Dynamique par Résonance Magnétique, URA CEA/CNRS 331, 91191Gif-sur-Yvette, France, and CNRS, École Normale Supérieure de Lyon, Laboratoire de Chimie, 46 Allée d'Italie, F-69364 Lyon, France*

*Received: August 19, 2008; Revised Manuscript Received: September 2, 2008*

The interaction of xenon with cryptophane derivatives is analyzed by NMR by using either thermal or hyperpolarized noble gas. Twelve hosts differing by their stereochemistry, cavity size, and the nature and the number of the substituents on the aromatic rings have been included in the study, in the aim of extracting some clues for the optimization of $^{129}$Xe-NMR based biosensors derived from these cage molecules. Four important properties have been examined: xenon-host binding constant, in-out exchange rate of the noble gas, chemical shift, and relaxation of caged xenon. This work aims at understanding the main characteristics of the host−guest interaction in order to choose the best candidate for the biosensing approach. Moreover, rationalizing xenon chemical shift as a function of structural parameters would also help for setting up multiplexing applications. Xenon exhibits the highest affinity for the smallest cryptophane, namely cryptophane-111, and a long relaxation time inside it, convenient for conservation of its hyperpolarization. However, very slow in−out xenon exchange could represent a limitation for its future applicability for the biosensing approach, because the replenishment of the cage in laser-polarized xenon, enabling a further gain in sensitivity, cannot be fully exploited.

## Introduction

Cryptophanes are hollow molecules made of two cyclotribenzylene (CTB) units linked by alkyldioxy chains of various lengths.[1] They can form host/guest complexes with small neutral molecules and form the most stable complexes with xenon observed so far. The smallest cryptophane was recently synthesized (**1**) and shows a tremendous affinity for xenon, thus prompting a renewal of interest in cryptophane gas trapping behavior.[2] It is the latest member of a large family of molecular hosts, the generic structure of which is depicted in Table 1, that vary in the length of the alkoxy linkers (cryptophane-A (**2**),[3] cryptophane-223 (**3**),[4] cryptophane-233 (**4**),[4] cryptophane-224 (**5**),[4] and cryptophane-E (**6**)[5]), in the substituents on the aromatic rings (**7**−**10**), and in the stereochemistry of the alkoxy linkers (cryptophane-C (anti) (**11**)[6] and cryptophane-D (syn) (**12**).[6]

Three effects can be observed in the $^{129}$Xe NMR spectra of xenon−cryptophane complexes. First, because of the high polarizability of the xenon electronic cloud, the chemical shift of xenon can span several hundreds ppm depending on its local environment. Second and as a consequence, in the vast majority of experimental conditions, a slow exchange on the xenon chemical-shift time scale occurs, and two signals are observable, corresponding to free xenon (approximately 200 ppm downfield from the external reference given by the gas resonance at quasi-null pressure) and xenon bound to the cryptophane (in the 30−80 ppm region). Third, the xenon signal can be enhanced by 4−5 orders of magnitude through optical pumping. Because of this set of favorable physical properties, xenon−cryptophane complexes constitute a good starting point for biosensing applications based on high-resolution NMR[7] or chemical-shift imaging.[8] For such applications, the host is modified to bear a tethered ligand that is designed to recognize specific biological receptors and thus to drag xenon to these receptors.[9] The important benefits of this approach are clearly the host affinity for xenon but also the multiplexing capability of $^{129}$Xe MRI that can be offered by chemical modification of the cage. The availability of xenon carriers bearing different recognition

**TABLE 1: Structure of the Cryptophanes 1−12 Considered in this Study[a]**

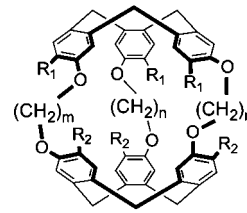


anti-cryptophanes
**1-11**

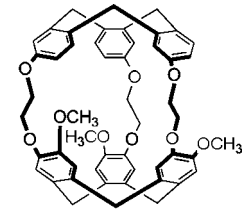


syn-cryptophane-D
**12**

| compound | *n* | *m* | $R_1$ | $R_2$ | usual name | reference |
|---|---|---|---|---|---|---|
| **1** | 1 | 1 | H | H | Cryptophane-111 | 2 |
| **2** | 2 | 2 | $OCH_3$ | $OCH_3$ | Cryptophane-A | 3 |
| **3** | 2 | 3 | $OCH_3$ | $OCH_3$ | Cryptophane-223 | 4 |
| **4** | 3 | 2 | $OCH_3$ | $OCH_3$ | Cryptophane-233 | 4 |
| **5** | 2 | 4 | $OCH_3$ | $OCH_3$ | Cryptophane-224 | 4 |
| **6** | 3 | 3 | $OCH_3$ | $OCH_3$ | Cryptophane-E | 5 |
| **7** | 2 | 2 | H | H | | |
| **8** | 2 | 2 | H | OBn | | |
| **9** | 2 | 2 | OBn | OBn | | |
| **10** | 2 | 2 | OBu | OBu | | |
| **11** | 2 | 2 | H | $OCH_3$ | Cryptophane-C | 6 |
| **12** | 2 | 2 | H | $OCH_3$ | Cryptophane-D | 6 |

[a] Compound **12** is the syn-isomer of compound **11**. Bn, benzyl group; Bu, butyl group.

* To whom correspondence should be addressed. E-mail: Patrick.Berthault@cea.fr.
[†] CEA, IRAMIS.
[‡] CNRS, École Normale Supérieure de Lyon.

10.1021/jp807425t CCC: $40.75 
Published on Web 10/17/2008

**SCHEME 1: Synthesis of Cryptophanes 9 and 10 from 15**

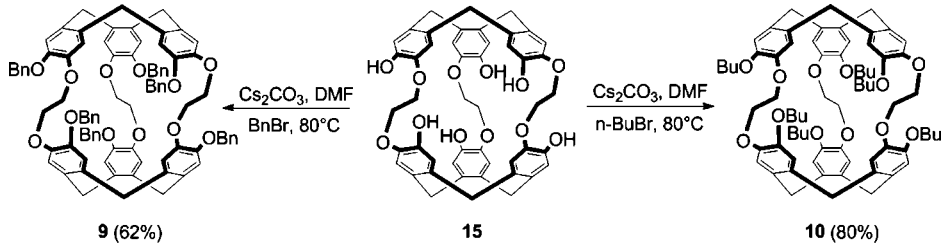


antennae will enable the detection of correlated biological events. With this approach, careful design of the host architecture can provide different chemical shifts for caged xenon, thereby giving each recognition antenna a unique signature.

Obviously, rational development would benefit from a detailed study of the host−xenon interactions for families of cryptophanes differing by size or the nature of the substituents. In this paper, several key parameters are examined, including (i) the affinity of xenon for the cryptophane cage, as defined by the binding constant, (ii) the chemical shift of caged xenon for various cryptophanes, with the objective of performing multiplexing experiments, (iii) the xenon in−out exchange rate, which should be slow on the xenon chemical-shift time scale but fast enough for a continuous refilling of the cage by laser-polarized xenon, and (iv) the longitudinal relaxation time which will affect the ability to maintain the polarization of xenon atoms in the cage. Therefore, the influence of the cryptophane isomerism, the cryptophane size, and the number and nature of the aromatic ring substituents on some of these experimental parameters has been examined for 12 cryptophanes, **1**−**12**, which are soluble in organic solvents and the structures of which are given in Table 1.

**SCHEME 2: Synthesis of Cryptophane 7 from Cryptophane 11**

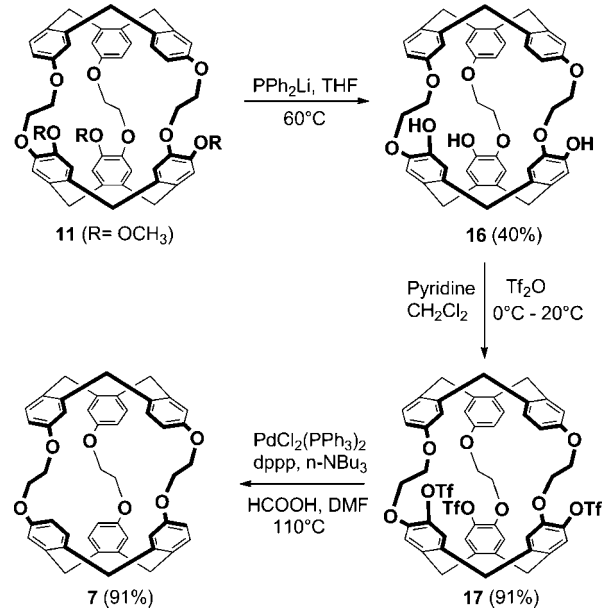


## Materials and Methods

Xenon in natural isotopic proportions was obtained from Air Liquide, and xenon enriched at 96% in isotope 129 was obtained from Chemgas. 1,1,2,2-tetrachloroethane-$d_2$ (99.60% deuterium), dichloromethane-$d_2$ (99.96% deuterium), chloroform-d (99.80% deuterium), and 1,2-dichloroethane-$d_4$ (99% deuterium) were from Eurisotop. Carbon tetrachloride was from Janssen and 1,2-dibromoethane from Fluka.

**Synthesis of Cryptophanes.** In contrast to the synthetic route published recently,[2] a novel approach is used for the synthesis of cryptophane **1**, which provides the cycloanisylene unit **13** in a single step (6% yield) and cryptophane **1** in two further steps (see Figure S1 in the Supporting Information). These two synthetic steps require a removal of the methoxy moieties with boron tribromide to give rise to the cyclotriphenolene, **14**, followed by the reaction of **14** with 1.5 equivs of bromochloromethane to give cryptophane **1** in 19% yield. Cryptophanes **2**−**6** were prepared according to published procedures using the template method.[4,5,10] Cryptophane **8** was prepared from a multistep synthesis according to a known experimental procedure.[11] New cryptophanes **9** and **10** were synthesized in good yield from cryptophanol **15** by using benzylbromide or 1-bromobutane in the presence of $Cs_2CO_3$ in DMF, respectively (see Scheme 1). Cryptophanes **11** and **12** were both synthesized in a single step by using scandium triflate as a catalyst.[11]

Cryptophane **7** was prepared by using a three-step synthetic route from cryptophane **11** (32% overall yield). Cryptophane **11** was first allowed to react with lithium diphenylphosphide in THF to give the cryptophanol **16** in moderate yield (nonoptimized: 40%). This moderate yield does not reflect the efficiency of the reaction but rather the difficulty of extracting and purifying **16**, which exhibits a very low solubility in both organic and aqueous media. This compound was then reacted with a slight excess of triflic anhydride in the presence of pyridine in $CH_2Cl_2$ at 0 °C to give cryptophane **17** with 91% yield (Scheme 2). Reduction of the triflate moieties was achieved by using a mixture of palladium dichloride diphenylphosphine, 1,3-diphenylphosphine propane (dppp), tris-*n*-butylamine (*n*-$NBu_3$), and formic acid in DMF at 110 °C according to a known procedure.[1] The procedure was very efficient for the reduction of hindered triflate groups, as observed recently for a cryptophane bearing a single triflate moiety.[12] Cryptophane **7** was thus obtained with a good yield after purification by chromatography on silica gel (91%).

***2,7,12-Trimethoxy-10,15-dihydro-5H-tribenzo[a,d,g]cyclononene (13).*** 3-Methoxy benzyl alcohol (13.13 g, 95.1 mmol) was added to a stirred mixture of $P_2O_5$ (21 g, 147 mmol) in dry $Et_2O$ (450 mL); a weak reflux was observed. Stirring was stopped, and the mixture was heated to 48 °C overnight. The $Et_2O$ solution was poured into a separatory funnel, and the $P_2O_5$ was washed with $CH_2Cl_2$ (3 × 220 mL). The organic layers were combined, and their volume was reduced by rotary evaporation, then washed with $H_2O$ (2 × 220 mL), by adding brine (80 mL) each time. The combined aqueous layers were extracted with $CH_2Cl_2$, and the organic layers were combined and dried over $Na_2SO_4$. The solvent was removed under reduced pressure to provide a pale yellow wax. Column chromatography ($CH_2Cl_2$/pentane 3:2), followed by rinsing the solid placed on a fritted filter with $Et_2O$, gave **13** as a white powder (6% yield).[11,13,14] $^1$H NMR (200 MHz, $CDCl_3$, 20 °C) $\delta$ 7.28 (d,

portion of signal hidden by $CDCl_3$ signal, 3 H, Ar), 6.86 (d, $^4J(H,H) = 2.7$ Hz, 3 H, Ar), 6.63 (d of d, $^3J(H,H) = 8.5$ Hz, $^4J(H,H) = 2.7$ Hz, 3 H, Ar), 4.73 (d, $^2J(H,H) = 13.5$ Hz, 3 H, $H_a$), 3.72 (s, 9 H; $OCH_3$), 3.62 (d, $^2J(H,H) = 13.6$ Hz, 3 H, $H_e$).

***10,15-Dihydro-5H-tribenzo[a,d,g]cyclononene-2,7,12-triol (14).*** Boron tribromide (37.0 mL of a 1 M solution of $BBr_3$ in $CH_2Cl_2$) was added dropwise to a solution of 2,7,12-trimethoxy-10,15-dihydro-5*H*-tribenzo[*a,d,g*]cyclononene (2.5 g, 6.9 mmol) in dry $CH_2Cl_2$ (64 mL) at −78 °C, and the solution was stirred for 5 min, before being warmed to room temperature and stirred overnight. The solution was poured onto an ice and $H_2O$ slurry. $H_2O$, then acetone (200 mL) and $CH_2Cl_2$ (200 mL), were added, and the solution was transferred to a separatory funnel. The organic layer was washed with $H_2O$ (1 × 170 mL). The combined aqueous layers were extracted with $CH_2Cl_2$ (180 mL) and acetone (30 mL). The combined organic layers were dried over $Na_2SO_4$. The solvent was removed under reduced pressure to provide a beige solid. Column chromatography ($CH_2Cl_2$/acetone 3:2) provided an off-white powder (95% yield).[13,14] Additionnal information: $^1$H NMR (200 MHz, acetone-$d_6$, 20 °C) $\delta$ 7.21 (d, 3H, $^3J(H,H) = 8.0$ Hz, Ar), 6.88 (d, 3 H, $^4J(H,H) = 2.6$ Hz, Ar), 6.55 (dd, 3H, $^3J(H,H) = 8.0$ Hz, $^4J(H,H) = 2.6$ H, Ar), 4.78 (d, 3 H, $^2J(H,H) = 13.4$ Hz, $H_a$), 3.55 (d, 3 H, $^2J(H,H) = 13.4$ Hz, $H_e$).

***Cryptophane* 1.** 10,15-Dihydro-5*H*-tribenzo[*a*,*d*,*g*]cyclononene-2,7,12-triol (1.01 g, 3.14 mmol) was placed in a flask containing dry $Cs_2CO_3$ (9.65 g, 0.34 mmol); then, dry DMF (40 mL) was cannulated into the flask, and the mixture was heated to 60 °C under stirring. $BrCH_2Cl$ (0.73 g, 0.37 mL) in DMF (100 mL) was placed in a dropping funnel, and 1−2 drop/min of the solution was added to the mixture at 60 °C; stirring was continued overnight after addition was complete. TLC (9:1 $CH_2Cl_2$/acetone) indicated no starting material remained. DMF was removed while heating under reduced pressure. $CH_2Cl_2$ (220 mL) and $H_2O$ (300 mL) were added to the beige solid. The aqueous layer was extracted with $CH_2Cl_2$ (2 × 240 mL), and the organic layers were combined and washed with $H_2O$ (250 mL). The combined organic layers were dried over $Na_2SO_4$. The solvent was removed under reduced pressure to provide an ochre solid. Column chromatography ($CH_2Cl_2$/acetone gradient 98:2 to 70:30), was followed by a second column ($CHCl_3$: 100%). Then, the white solid was rinsed with $Et_2O$ onto a fritted filter to provide a white powder. Yield 19%. Decomposes above 200 °C; $^1$H NMR (500 MHz, $CDCl_3$, 20 °C) $\delta$ 6.967 (s broad, 6 H, Ar), 6.724 (s broad, 6 H; Ar), 6.570 (s broad, 6 H; Ar), 5.71 (s, 6 H; $OCH_2O$), 4.48 (d, 6H, $^2J(H,H) = 13.5$ Hz; $H_a$), 3.41 (d, 6H, $^2J(H,H) = 13.5$ Hz; $H_e$); $^{13}$C NMR ($CDCl_3$) $\delta$ = 157.77 (6 C, Ar), 140.76 (6 C, Ar), 132.13 (6 C, Ar), 129.85(6 C, Ar), 117.59 (6 C, Ar), 111.68 (6C, Ar), 86.17 (3C, O$\underline{C}H_2$O), 35.30 (6 C, $\underline{C}_{a,e}$); IR (KBr pellet) 754, 827, 1039, 1149, 1232, 1300, 1321, 1421, 1441, 1498, 1579, 1604, 2920, 2983 $cm^{-1}$; UV (hexanes) ($\lambda$) 242 nm (16 800 L $mol^{-1}$ $cm^{-1}$), 279 nm (5 500 L $mol^{-1}$ $cm^{-1}$), 288 nm (6 900 L $mol^{-1}$ $cm^{-1}$); HRMS (TOF MS ES+) *m*/*z* calcd for $C_{45}H_{36}O_6Na$ 695.2410; found 695.2397.

***Cryptophan-ol (16).*** Lithium diphenyphosphide 1 M (3.4 mL, 3.35 mmol) was added dropwise to a stirred mixture of cryptophane **11** (0.25 g, 0.3 mmol) in dry THF (5 mL). The resulting red mixture was stirred overnight at 60 °C under an argon atmosphere. The mixture was then poured in water and extracted three times with $CH_2Cl_2$. The combined organic layers were washed three times with brine and dried over $Na_2SO_4$. Filtration and evaporation of the solvent leaves compound **16** as a white residue, which was purified through a short column of silica gel ($CH_2Cl_2$/acetone: 90/10 then 80/20). Evaporation of the solvent gives compound **16** as a white product, which was washed on a frit with $Et_2O/CH_2Cl_2$ (50/50), then with pure $Et_2O$. This procedure gives rise to compound **16** (0.09 g; 40%) as a white solid. Mp: 296 °C. $^1$H NMR (500 MHz, $CDCl_3$, 20 °C): $\delta$ = 7.10 (d, 3H, $^3J(H,H) = 8.5$ Hz; Ar), 6.73 (d, 3H, $^4J(H,H) = 2.6$ Hz; Ar), 6.67 (s, 3H; Ar), 6.52 (s, 3H; Ar), 6.37 (dd, 3H, $^3J(H,H) = 8.5$ Hz, $^4J(H,H) = 2.6$ Hz; Ar), 5.28 (s, 3H; OH), 4.59 (d, 3H, $^2J(H,H) = 13.6$ Hz; $H_a$), 4.52 (d, 3H, $^2J(H,H) = 13.6$ Hz; $H_a$), 4.40−4.30 (m, 6H; $CH_2$), 4.28−4.25 (m, 3H; $CH_2$), 3.86−3.82 (m, 3H; $CH_2$), 3.51 (d, 3H, $^2J(H,H) = 13.6$ Hz; $H_e$), 3.31 (d, $^2J(H,H) = 13.6$ Hz, 3H, $H_e$). $^{13}$C NMR (126.7 MHz, $CDCl_3$, 20 °C) $\delta$ = 154.9 (3C), 144.6 (3C), 144.5 (3C), 140.8 (3C), 133.0 (3C), 131.1 (3C), 130.8 (3C), 130.7 (3C), 119.2 (3C), 115.0 (3C), 114.1 (3C), 109.5 (3C), 67.3 (3C; $OCH_2$), 64.5 (3C; $OCH_2$), 35.8 (3C; $C_{a,e}$), 35.6 (3C; $C_{a,e}$). HRMS (LSIMS), calcd for $C_{48}H_{42}O_9Na$ [$M^{\circ+}$], 785.2727; found 785.2736.

***Cryptophane* 17.** Triflic anhydride (0.25 g, 0.15 mL) was added dropwise at 0 °C to a stirred solution of cryptophan-ol **16** (0.076 g, 0.1 mmol) in pyridine (2 mL) and $CH_2Cl_2$ (2 mL). The orange solution was stirred overnight at 20 °C and then poured in water. The product was extracted three times with $CH_2Cl_2$. The combined organic layers were washed with brine and dried over $Na_2SO_4$. Evaporation of the solvent under reduce pressure leaves a red residue. Purification by chromatography on silica gel ($CH_2Cl_2$/acetone: 90/10) gives cryptophane **17** as a white glassy product (0.105 g, 91%). Decomposes above 300 °C. $^1$H NMR (500 MHz, $CDCl_3$, 20 °C): $\delta$ = 7.10 (d, 3H, $^3J(H,H) = 7.0$ Hz; Ar), 7.00 (s, 3H; Ar), 6.76 (s, 3H; Ar), 6.66 (s, 3H; Ar), 6.39 (d, 3H, $^3J(H,H) = 7.0$ Hz; Ar), 4.60 (d, $^2J(H,H) = 14.0$ Hz, 3H; $H_a$), 4.57 (d, 3H, $^2J(H,H) = 14.0$ Hz, $H_a$), 4.40−4.25 (m, 9H; $CH_2$), 3.97 (m, 3H; $CH_2$), 3.50 (d, 3H, $^2J(H,H) = 14.0$ Hz; $H_e$), 3.46 (d, 3H, $^2J(H,H) = 14.0$ Hz; $H_e$). $^{13}$C NMR (126.7 MHz, $CDCl_3$, 20 °C) $\delta$ = 155.6 (3C), 149.4 (3C), 140.8 (3C), 139.5 (3C), 131.3 (3C), 131.2 (3C), 131.1 (3C), 123.4 (3C), 119.6 (3C), 118.9 (q, 3C, $^1F(C,F) = 324.0$ Hz, $CF_3$), 117.0 (3C), 110.3 (3C), 67.4 (3C; $OCH_2$), 64.3 (3C; $OCH_2$), 36.1 (3C; $C_{a,e}$), 35.8 (3C; $C_{a,e}$). HRMS (LSIMS), calcd for $C_{51}H_{39}O_{15}F_9S_3Na$ [$M^{\circ+}$] 1181.1205; found 1181.1136.

***Cryptophane* 7.** Cryptophane **17** (0.1 g, 0.086 mmol), $PdCl_2(PPh_3)_2$ (0.061 g, 0.086 mmol), dppp (0.071 g, 0.17 mmol), DMF (1.5 mL), $NBu_3$ (1 mL), and formic acid (0.1 mL) were added in this order to a 5 mL round-bottom flask. The mixture was stirred overnight at 110 °C under an argon atmosphere; then, the mixture was poured in a mixture of $CH_2Cl_2$ and water. The product was extracted three times with a small amount of $CH_2Cl_2$. The combined organic layers were washed once with brine and then dried over $Na_2SO_4$. Filtration and evaporation of the solvent under reduced pressure leaves a dark red residue (at the end, the vacuum pump is necessary to remove the $NBu_3$). Cryptophane **7** is isolated by column chromatography ($CH_2Cl_2$/acetone: 90/10). The solid is washed on a frit with diethyl ether to give compound **7** as white crystals (0.056 g, 91%). Decomposes above 300 °C. $^1$H NMR (500 MHz, $CDCl_3$, 20 °C): $\delta$ = 7.09 (d, 6H, $^3J(H,H) = 8.5$ Hz; Ar), 6.66 (d, 6H, $^4J(H,H) = 2.5$ Hz; Ar), 6.48 (dd, 6H, $^3J(H,H) = 8.5$ Hz, $^4J(H,H) = 2.5$ Hz; Ar), 4.62 (d, 6H, $^2J(H,H) = 13.5$ Hz; $H_a$), 4.17 (m, 12H; $OCH_2$), 3.48 (d, 6H, $^2J(H,H) = 13.5$ Hz, $H_e$). $^{13}$C NMR (126.7 MHz, $CDCl_3$, 20 °C) $\delta$ = 156.6 (6C), 140.7 (6C), 131.4 (6C), 130.6 (6C), 116.8 (6C), 113.3 (6C), 65.2 (6C; $OCH_2$), 36.2 (6C; $OCH_2$). HRMS (LSIMS), calcd for $C_{48}H_{42}O_6Na$ [$M^{\circ+}$] 737.2879; found 737.2883.

***Cryptophane* 9.** Benzyl bromide (0.22 g, 0.2 mL, 1.98 mmol) was added to a stirred solution of cryptophan-ol **15** (0.1 g, 0.12 mmol), $Cs_2CO_3$ (0.28 g, 0.86 mmol) in DMF (3.5 mL). The mixture was stirred for 48 h at 80 °C under an argon atmosphere. The mixture was poured in water and extracted three times with $CH_2Cl_2$. The combined organic layers were washed three times with brine and then dried over $Na_2SO_4$. Evaporation under reduced pressure left a residue, which was passed through a column of silica gel ($CH_2Cl_2$/acetone: 90/10). Several fractions containing the product were evaporated under reduced pressure to give cryptophane **9** as a white glassy product. Recrystallization in a mixture of $CHCl_3$ and EtOH gave **9** (0.1 g; 62%) as white crystals. Mp: 170 °C. $^1$H NMR (500 MHz, $CDCl_3$, 20 °C): $\delta$ = 7.3−7.2 (m, 15H; Bn), 6.77 (s, 6H; Ar), 6.70 (s, 6H; Ar), 4.78 (m, 12H; $OCH_2$), 4.52 (d, 6H, $^2$J(H,H) = 13.5 Hz; $H_a$), 4.3−4.2 (m, 12H; $OCH_2$), 3.33 (d, 6H, $^2$J(H,H) = 13.5 Hz; $H_e$). $^{13}$C NMR (126.7 MHz, $CDCl_3$, 20 °C) $\delta$ = 149.0 (6C), 147.5 (6C), 137.1 (6C), 134.2 (6C), 132.7 (6C), 128.4 (12C), 127.8 (6C), 127.4 (12C), 121.8 (6C), 117.8 (6C), 71.8 (6C; $OCH_2$), 69.6 (6C; $OCH_2$), 36.2 (6C; $C_{a,e}$). HRMS (LSIMS), calcd for $C_{90}H_{78}O_{12}N_a$ [$M^{\cdot+}$] 1373.5391; found 1373.5315.

***Cryptophane* 10.** Cryptophan-ol **15** (0.1 g, 0.12 mmol), $Cs_2CO_3$ (0.48 g, 1.47 mmol), and DMF (6 mL) were placed in a three-neck flask equipped with a reflux condenser. Then, 1-bromobutane (0.152 g, 0.12 mL, 1.1 mmol) was added in one portion. The mixture was stirred overnight at 80 °C under an argon atmosphere and then poured in water. The product was extracted three times with $CH_2Cl_2$. The combined organic layers were washed several times with brine and dried over $Na_2SO_4$. Filtration followed by evaporation of the solvent under reduced pressure leaves a residue that was purified by column chromatography ($CH_2Cl_2$/acetone: 90/10) to provide cryptophane **10** as a white glassy product. Recrystallization in a mixture of $CHCl_3$ and EtOH gave cryptophane **10** as white crystals (0.11 g; 80%). Mp: 281 °C. $^1$H NMR (500 MHz, $CDCl_3$, 20 °C): $\delta$ = 6.72 (s, 6H; Ar), 6.66 (s, 6H; Ar), 4.53 (d, 6H, $^2$J(H,H) = 13.5 Hz; $H_a$), 4.15 (m, 6H), 4.05 (m, 6H), 3.94 (m, 6H), 3.80 (m, 6H), 3.36 (d, 6H, $^2$J(H,H) = 13.5 Hz; $H_e$), 1.75 (p, 12H, $^3$J(H,H) = 7.0 Hz; $CH_2$), 1.54 (m, 12H, $^3$J(H,H) = 7.0 Hz; $CH_2$), 1.03 (t, 18H, $^3$J(H,H) = 7.0 Hz; $CH_3$). $^{13}$C NMR (126.7 MHz, $CDCl_3$, 20 °C) $\delta$ = 149.6 (6C), 147.4 (6C), 134.5 (6C), 132.1 (6C), 122.3 (6C), 117.0 (6C), 69.7 (6C), 69.4 (6C), 36.2 (6C), 31.8 (6C), 19.4 (6C), 14.1 (6C). HRMS (LSIMS), calcd for $C_{72}H_{90}O_{12}Na$ [$M^{\cdot+}$] 1169.6330; found 1169.6333.

**Characterization of the Compounds.** The synthesized cryptophanes were characterized by mass spectrometry (HRMS LSIMS) performed by the Centre de Spectrométrie de Masse, University of Lyon, on a Thermo-Finnigan MAT 95XL spectrometer, and by $^1$H and $^{13}$C NMR spectra recorded on Varian Unity 500, Bruker Avance II 500 spectrometers. Chemical shifts, $\delta$($^1$H, $^{13}$C), are given relative to $Me_4Si$. Column chromatographic separations were carried out on Merck silica gel 60 (0.040−0.063 mm). Analytical thin layer chromatography (TLC) was performed on Merck silica gel TLC plates F-254. Melting points were measured on a Perkin-Elmer DSC7 calorimeter. Solvents were distilled prior to use: DMF and $CH_2Cl_2$ from $CaH_2$, pyridine from KOH, and THF and $Et_2O$ from Na/benzophenone ketyl. Lithium diphenylphosphide was freshly prepared from a known procedure.[15]

In order to remove the remaining solvent traces before the xenon binding experiments, the cryptophanes powders were heated at 70 °C under vacuum during 1−2 h.

**Xenon Polarization.** Prior to measurement of $^{129}$Xe spectra, xenon was polarized by optical pumping, by using the spin-exchange method,[16,17] to approximately 30% via our home-built apparatus.[18] Briefly, the $D_1$ electronic transition of rubidium was excited by using a tunable titanium:sapphire laser, producing approximately 6 W continuous power when pumped by a 25 W argon ionized laser. The light crossed a beam expander, a beam splitter cube and a $\lambda$/4 plate, ensuring purely circularly polarized light. Then, the beam reached the pumping cell containing 0.13−2.7 kPa xenon, 27 kPa nitrogen, and some droplets of rubidium, partially vaporized by heating to approximately 368 K. After approximately 10 min of optical pumping, hyperpolarized xenon was condensed in a tube immersed in liquid nitrogen, in a magnetic field of 0.3 T created by a solenoid, whereas gaseous nitrogen was evacuated toward a pump. The xenon was then transported to the NMR spectrometer.

**Sample Preparation and NMR Spectroscopy.** Unless otherwise specified, individual cryptophanes or mixtures of cryptophanes were dissolved in 1,1,2,2-tetrachloroethane-$d_2$ in the 1−25 mM range, depending on the parameter to be measured. Samples were degassed by several freeze−pump−thaw cycles. Polarized or thermal xenon was then added to the NMR tube by condensation (by means of a hollow spinner filled with liquid nitrogen) or by expansion, according to the desired final xenon pressure in the NMR tube. NMR spectra dedicated to the characterization of xenon−cryptophane binding were recorded on a 11.7 T Bruker Avance II spectrometer equipped with either a Bruker broadband inverse 5 mm probehead or a Nalorac broadband direct 5 mm probehead.

**Xenon−Cryptophane Binding Constant Determination.** The xenon−cryptophane binding constant for **2**[19] and **6**[4] had been determined by using a 1:1 stoechiometry (only one xenon atom able to enter in the cage). This assumption may be safely extended to all other cryptophanes reported here, because their cavity volume is smaller than that of **6**. Although other parameters, such as the nature of the solvent, influence xenon−cryptophane binding, an apparent binding constant $K_i$ may be defined as $K_i = [Xe@C_i]/[Xe][C_i]$, where $[C_i]$ and $[Xe@C_i]$ are the concentrations of the free and bound forms of cryptophane $i$, respectively, enabling comparisons between cryptophanes in the same solvent.

The Xe@**1** binding constant at 278 K was evaluated by following the same method as that previously used at 293 K,[2] that is, by competition with **2**. We took advantage of slow-exchange conditions between certain proton signals of the occupied and free cages of **1**. A solution of 8.4 mM of **1** and 10.2 mM of **2** was degassed in the NMR tube. Then, xenon gas was added while the tube was maintained at about 193 K in a cold methanol bath, in order to drastically reduce the solvent vapor pressure without freezing xenon. After a delay sufficient for temperature equilibration, $^1$H and $^{129}$Xe spectra were recorded under quantitative conditions. It can be demonstrated that the ratio $K_1/K_2$ is independent of xenon solubility and is given by equation 1

$$K_{Xe@1}/K_{Xe@2} = [\gamma(1+\beta)/\alpha] - \beta \qquad (1)$$

where $\alpha$ is defined as the concentration ratio of cryptophanes **1** and **2,** $\beta$ is defined as the ratio of cryptophane **1** containing a xenon atom to empty cryptophane **1**, and $\gamma$ is defined as the concentration ratio of cages **1** and **2** containing xenon atoms. The $\alpha$ term was determined through integration of the aromatic signals of the **1** + **2** solution mixture, and $\beta$ was obtained from integration of the aromatic protons at approximately 7.05 ppm on the $^1$H spectrum of **1** (the doublet assigned to filled cages is shifted downfield by approximately 0.03 ppm compared to that

assigned to empty cages, data not shown). The $\gamma$ term was determined from the thermally polarized xenon spectra of the mixture. The binding constant value of 3900 $M^{-1}$ for Xe@**2** was taken from ref 19.

The Xe@**7** binding constant was evaluated from the measurement of the proton chemical shifts of **7** upon varying the amount of bound xenon. In an NMR tube containing a reservoir, 190 $\mu$L of a 6.2 mM solution of **7** in 1,1,2,2-tetrachloroethane-$d_2$ was placed. The solution was thoroughly degassed, and an initial proton spectrum was acquired. Then, a series of known amounts of xenon were added into the NMR tube by measuring the decrease of pressure in a known volume through a membrane gauge, while the solution is maintained frozen by immersion in a liquid nitrogen bath. After xenon sublimation, the tube was laid horizontally for 5 min with the solution in the reservoir in order to increase the gas−liquid interface, at a temperature close to that of the NMR study. Then, the NMR tube was inserted into the spectrometer. The gas−liquid equilibrium of xenon was reached after approximately 10 min, because the proton chemical shifts did not evolve anymore, as observed through a series of proton spectra. For each experimental point, the proportion of xenon in the gas phase, free in solution and encapsulated in **7** depended on the xenon molar solubility and the Xe@**7** binding constant. Only the solubility value at 298 K was known.[20] However, the variation of the molar fraction of dissolved xenon with temperature at atmospheric pressure, from which molar solubility could be deduced from the knowledge of the molar volume of the solvent, is known for a wide set of solvents.[21−25] For a given gas, this variation was fitted according to a currently used parametric law[25] (data not shown), and the ratio of molar fractions at 278 and 298 K was extracted. Except for water, this ratio was between 1.15 and 1.39. A value of 1.27 ± 0.13 was then used. As 1,1,2,2-tetrachloroethane density increases by about 1.3% between 303.15 and 293.15 K,[26] it has been estimated to increase by 2.6% between 298 and 278 K. Finally, solubility at 278K has been estimated as 1.29 ± 0.13 $\mu$M $Pa^{-1}$. The binding constant was then evaluated by fitting the chemical shift of an aromatic proton, which reflects the proportion of cages filled by a xenon atom relative to the amount of added xenon (see figure S2 in the Supporting Information). The accuracy of the measurement depends strongly on the accuracy of the xenon quantity added into the tube, especially for very low pressures that do not imply a saturation of all cages. The presence of the reservoir provided the possibility to reach an equilibrium pressure of only 36 Pa after the addition of 0.14 micromoles of xenon. An error for the chemical-shift determination of 1.4 ppb has been estimated from the calculation of reduced $\chi^2$ from the model. By using relative errors from 2 to 10% on each experimental parameter, except 0.1% for temperature and 1.4 ppb for chemical shifts, the median and standard deviation of $K_7$ were deduced through a Monte Carlo simulation repeated 10 000 times.

The Xe@**5** binding constant was evaluated according to the same method, by using the most downfield-shifted aromatic proton signal. The error in chemical-shift determination has been estimated as 1.9 ppb.

**Chemical Shifts.** The $^{129}$Xe chemical shifts were calibrated through the resonance signal of xenon in tetrachloroethane-$d_2$. Segebarth et al.[20] precisely measured the xenon chemical shifts in this solvent as 223.60 ppm at 298 K, relative to the resonance of xenon gas extrapolated to zero pressure. They also observed that the chemical shift of dissolved xenon does not significantly depend on pressure.

The in−out kinetics of xenon slightly influences its chemical shift. The difference between the observed value and that estimated in the case of infinitely slow exchange has been assessed through a two-site model with unequal population.[27] In a very unfavorable situation, reported in Figure S2 in the Supporting Information for cryptophane **7**, the chemical-shift discrepancy of encapsulated and free xenon does not exceed 0.5 ppm. For **2** at the highest experimental temperature, the error of the uncorrected chemical-shift value is on the order of 0.01 ppm. This is much lower than the uncertainties due to sample temperature calibration. Therefore, experimental chemical shifts were used without further correction. Moreover, the chemical shift of xenon in solvent was negligibly modified by the presence of a cryptophane in the solution. The linear dependence of this chemical shift with temperature, −315 ± 3 ppb/K, already reported by Bartik et al.,[19] was used to calibrate this signal at a chosen temperature for all cryptophanes. For some cryptophanes, for example, **12** and **7**, the calibration was performed at the lowest temperature.

Free xenon chemical shifts in $CDCl_3$ and $CD_2Cl_2$ at 293 K were taken by reference equal to 216 and 193 ppm, respectively, from their value at 296.5 K[28] and from the variation of the chemical shift of 1,1,2,2-tetrachloroethane-$d_2$ with temperature.

**Release Rate of Caged Xenon.** Slow exchange conditions on the xenon chemical-shift time scale were observed for all cryptophanes under the experimental conditions of host concentration (2−11 mM), xenon pressure ($3 \times 10^3$−$1.6 \times 10^5$ Pa), and temperature (240−355 K). The apparent xenon release rates were estimated by multiplying by $\pi$ the full width at half height of the signals assigned to bound xenon. The portion of the cages that did not contain a xenon atom is not negligible under certain experimental conditions. Therefore, the use of a quasi exclusive second-order mechanism to explain the line width of the bound-xenon signal[19] did not necessarily apply. However, the observed variation of the xenon line widths with xenon pressure revealed a second-order mechanism (degenerate state) for the xenon−cryptophane association that could be described by the following equilibrium:

$$\mathrm{Xe} @ \mathrm{C}_i + \mathrm{Xe}^* \rightleftarrows \mathrm{Xe}^* @ \mathrm{C}_i + \mathrm{Xe} \qquad (2)$$

A specific experimental protocol, in which samples contained a mixture of cryptophanes, was therefore chosen, using either hyperpolarized or thermally polarized xenon, in order to ensure a kinetic comparison under the same conditions of temperature and xenon pressure. The use of a solution containing several cryptophanes is not expected to modify the results as it was shown previously that the direct xenon exchange rate between cryptophane cages was negligible compared to the release rate into the solvent.[10]

***T*$_1$ Measurements.** The longitudinal relaxation times of xenon encapsulated in cryptophanes were measured by one of the two following methods. The first method consisted of monitoring the evolution of the xenon peak area of the xenon signals, either free in solvent or in the cage, obtained after very short excitation pulses. Because fast in−out exchange rates on the xenon $T_1$ time scale were present for all cryptophanes in our experimental conditions, an average $T_1$ was then deduced. As the longitudinal relaxation time of xenon free in 1,1,2,2-tetrachloethane-$d_2$ is very long, on the order of hundreds of seconds,[29] compared to that in cryptophanes (see below), its exact value has a negligible influence on the calculated $T_1$ value of bound xenon, which is therefore simply deduced from the ratio of the signal area of xenon in both environments.

In the second method, the classical inversion−recovery sequence was used with thermally polarized xenon. Both the

**TABLE 2: Binding Constants $K_i$ of Cryptophanes 1−7 with Xenon at 278 K in 1,1,2,2-Tetrachloroethane-$d_2$ and Calculated Internal Cavity Volume**

| | cryptophane | | | | | | |
|---|---|---|---|---|---|---|---|
| | **1** | **2** | **3** | **4** | **5** | **6** | **7** |
| $K_i$ ($M^{-1}$) | 28 000 ± 5000[a] | 3900 ± 500[b] | 2800[b] | 800[b] | 9.5 ± 1.0[c] | 5−10[a] | 1400 ± 150[a,c] |
| volume (Å$^3$) | 81[d] | 95[b] | 102[b] | 117[b] | 110[b] | 121[b] | n. m. |

[a] This work. [b] Reference 4. [c] See Figure S2 in the Supporting Information. [d] Reference 2; n. m., not measured.

noncomplete return to equilibrium and errors on the inversion and lecture pulse angles were taken into account in the calculation of $T_1$.

## Results and Discussion

With the goal of optimizing the cryptophane cage moiety for biological sensing applications, the influence of the structural and electronic properties of cryptophane on key parameters such as the xenon binding constant, chemical shift, in−out kinetics, and longitudinal relaxation is examined. This analysis is based on a set of 12 cryptophanes differing by their stereoisomerism, their length of the linkers, and the number and type of substituents on the aromatic rings. A comparative study within this set renders possible the formulation of hypotheses on the molecular origin of the differences observed for some xenon−cryptophane binding properties. Obviously, none of these cryptophanes is significantly soluble in water or blood and thus will not be directly amenable for xenon biosensing. The presence of a hydrophilic tether however will help solubilize the cage molecule in biological fluids. Nevertheless, this study aims at a better understanding of xenon−host interactions.

**Binding Constants.** The binding constants, $K_i$, of xenon with cryptophanes **1**−**7** in 1,1,2,2-tetrachloroethane-$d_2$ at 278 K are reported in Table 2. As already noticed, these average values compete favorably with those encountered for xenon in other cage molecules: for instance, values of 20 $M^{-1}$ for α-cyclodextrin in water at room temperature[30] and of 200 $M^{-1}$ for cucurbit[6]uril in acidic conditions[31] are reported. The exception is the very recent measurement of a binding constant of 3000 $M^{-1}$ for xenon in a cucurbit[6]uril derivative.[32] Anyway, cryptophanes seem really to be among the best candidates to constitute the core of xenon sensors.

Cryptophanes **2**−**6** differ only by the length of the alkyl chains linking the two CTB units. The decrease of the xenon binding constant value in the series **2**, **3**, **4**, and **6** may be explained by a decrease of stabilizing cryptophane−xenon interactions through London forces between the noble gas and the accessible atoms of the host. It has indeed been shown that xenon is stabilized by close proximity to ethanedioxy linkers in preference to longer alkyldioxy chains.[33] Also, cryptophane sampling of conformational space when binding xenon, or not, may vary in the series and affect the entropic part of $K_i$. The role of the solvent, which for large cavities can act as a competitor, could explain the low binding constant value for Xe@**5**, because this host has one butanedioxy and two ethanedioxy linkers. In this case, more flexible portals may allow increased interaction between solvent molecules and the encapsulated noble gas.

The binding constant of xenon with **1**, $K_1$, had previously been estimated as 10 000 $M^{-1}$ at 293 K, on the basis of competition experiments with **2**.[2] A $K_1$ value of 28 000 ± 5000 $M^{-1}$ at 278 K is now determined by using the same method. This is by far the highest binding constant between xenon and a cage molecule ever observed in an organic solvent. The already mentioned trend which indicates that the xenon−cryptophane affinity decreases as the cavity size increases (**2, 3, 4, 6** series)[4] is thus extended by one element: cryptophane **1**. With host **1**, the apparent linear relationship between the binding constant value and the cavity volume is broken (Table 2). For this cryptophane, the ratio of the volume of xenon and the volume of the cavity, $r = 0.52$, is very close to the optimal value of 0.55 given by Rebek[34] and significantly increases the affinity for the noble gas. It is noteworthy that the water-soluble congener of **1** would exhibit an even higher binding constant in this solvent because of the hydrophobic character of the xenon atom.

Clearly it can be argued that in contrast to **2**−**6**, cryptophane **1** has no methoxy groups on the aromatic rings, thereby questioning the validity of the comparison, because the electronic environment of the encapsulated xenon atom is significantly modified by the removal of the six methoxy groups. Therefore, the binding constant of xenon with **7** was also measured. Cryptophane **7** differs from **1** by the length of the linkers between the CTB bowls and differs from **2** by the absence of methoxy substituents on the aromatic rings in positions $R_1$ and $R_2$ (Table 1). The affinity of xenon for **7** is 20 times lower than that for **1** and 2.8 times lower than that for **2** (Table 2). It is unlikely that the change of cavity size resulting from the presence of methoxy groups instead of hydrogen atoms is solely responsible for the decrease of xenon affinity from **2** to **7** (otherwise, the affinity would be higher for **7** than for **3**). Rather, partial access of the solvent through the portals may act as a competitor to xenon in the case of **7**.

The estimated cavity volume of **5** ($V = 110$ Å$^3$) is smaller than that of **4** ($V = 117$ Å$^3$), whereas the binding constant is far lower (Table 2). This has been previously explained by a higher flexibility of **5**, which has a butanedioxy linker. Thus, some conformations unfavorable for xenon binding may exist for **5**.

**Xenon Chemical Shift.** Our observations confirm previous results,[19] which showed that neither cryptophane concentration nor xenon pressure significantly modify the chemical shift of xenon free in solution, as long as the slow exchange regime stands. The temperature dependence of the xenon chemical-shift values for xenon encapsulated in cryptophanes **1**−**12** are reported in Figure 1, at various temperatures. Let us first consider the xenon chemical-shift values at 293 K (dashed vertical line). The value for Xe@**12** will be extrapolated, because it has been measured at slightly lower temperature.

The arrangement of the O−$CH_2$−$CH_2$−O linkers has a strong influence on the chemical shift of encapsulated xenon. This is exemplified by a larger downfield xenon chemical shift for **12** than for **11**. It may be correlated with a different shape of inner space available for xenon, less spherical in **12** than in **11**, as observed by X-ray crystallography when a dichloromethane molecule is encapsulated.[6]

The decrease of xenon chemical shift observed with the increase of portal size in the **2, 3, 4, 6** series had been rationalized by ab initio calculations.[35] It was found that xenon is more deshielded upon closer approach to a host atom;

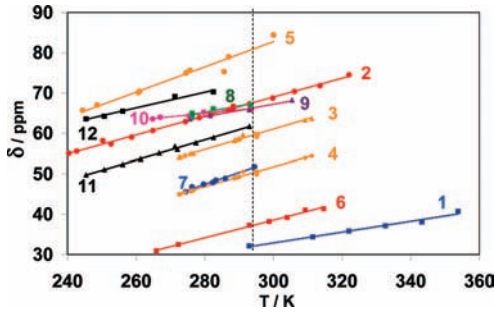


**Figure 1.** Chemical shift of xenon encapsulated in cryptophanes in $(CDCl_2)_2$ as a function of temperature for **1** (blue squares), **2** (red circles), **3** (orange triangles), **4** (orange diamonds), **5** (orange circles), **6** (red squares), **7** (blue circles), **8** (green squares), **9** (violet triangles), **10** (pink circles), **11** (black triangles), and **12** (black squares). Symbols: experimental data. Lines: linear fit of experimental points. The dashed vertical line corresponds to $T = 293$ K.

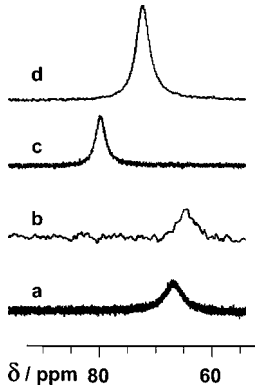


**Figure 2.** Hyperpolarized $^{129}$Xe spectrum of a solution of **2** in 1,1,2,2-tetrachloroethane-$d_2$ (a), chloroform-d (b), 1,2-dichloroethane-$d_4$ (c), and 1,2-dibromoethane (d), obtained in one scan at 293 K. Chemical shifts are referenced (a−c) to the signal of xenon free in solution[19,20,28] or (d) to a signal at 0 ppm assigned to gas bubbles (data not shown).

therefore, xenon in the largest cage (**6**) is the most upfield shifted. This does not apply to cryptophane **1**. However, it was recently reported that relativistic effects, that were neglected by Sears and Jameson,[35] may significantly influence xenon chemical shift in other cage molecules.[36,37]

Obviously, the nature of the substituents on the aromatic rings has its own influence on the chemical shift of encapsulated xenon. For instance, the difference in shift of approximately 20 ppm between Xe@**2** and Xe@**7** is easily explained by the absence of the methoxy groups in the latter complex, which leads to a decrease of the electronic density in the aromatic ring of **7** and therefore a larger shielding effect.

Comparison of two cryptophanes having the same substituents but different sizes, **1** and **7**, shows an unexpected shielding effect for the former, which could be explained by a solvent effect. In the present study, a detailed comparison of the $^{129}$Xe NMR parameters of the complexes is made in 1,1,2,2-tetrachloroethane-$d_2$ ($C_2D_2Cl_4$). However, it should be kept in mind that the solvent may also have its own influence on parameters such as the chemical shift of encapsulated xenon. As an example, $^{129}$Xe spectra of **1** and **2** were also recorded at 293 K in chloroform-d, 1,2-dichloroethane-$d_4$, and carbon tetrachloride (see Figures 2 and S3 in Supporting Information). The $^{129}$Xe spectra of **2** in dichloromethane-$d_2$ and 1,2-dibromoethane were also recorded. Two signals are observed in 1,2-dichloroethane, 1,1,2,2-tetrachloroethane, chloroform, and 1,2-dibromoethane, indicating a slow exchange on the chemical-shift time scale. For **2**, the signal

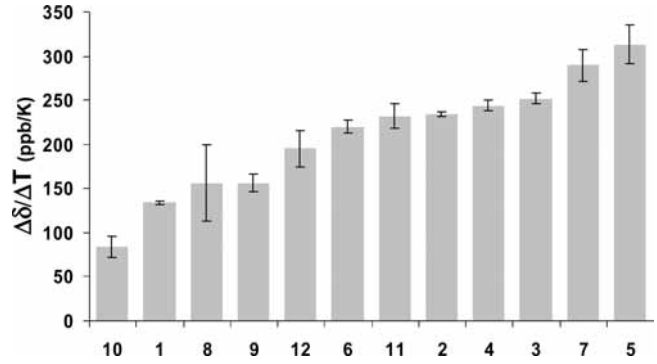


**Figure 3.** Temperature dependence of the chemical shift of xenon encapsulated in cryptophanes **1**−**12** in 1,1,2,2-tetrachloroethane-$d_2$ in ppb $K^{-1}$.

characteristic of bound xenon is downfield shifted by approximately 13 ppm in 1,2-dichloroethane and by 5 ppm in 1,2-dibromoethane compared to that in 1,1,2,2-tetrachloroethane, whereas it is only slightly upfield shifted by 2 ppm in chloroform. Conversely, the chemical shift of xenon in **1** is quasi independent of the nature of the solvent. The explanation we propose is that, in the case of **2** in $(CD_2Cl)_2$ and to a lesser extent in $(CD_2Br)_2$, a solvent molecule partially enters the cavity, leading to a downfield shift of the bound xenon signal. This does not occur in 1,1,2,2-tetrachloroethane where steric hindrance of each end of the molecule is increased by the presence of a second halogen atom, nor in chloroform which contains three chlorine atoms. For **1**, the halogenated solvent molecules are too big to enter—even partially—into the cavity, therefore giving rise to a quasi invariant chemical shift of bound xenon whatever the solvent. Moreover, xenon chemical shift in **1** is modified by less than 0.03 ppm when alkoxy linkers are deuterated (data not shown). This confirms both the conformation of linkers in **1**, that point outward the cavity, and confirms the low flexibility of this cryptophane.

The $^{129}$Xe spectra for **2** in dichloromethane and carbon tetrachloride reveal only one signal (data not shown). This clearly confirms that $CD_2Cl_2$ has a good affinity for the cavity of **2**,[38] inducing a far lower apparent binding constant for xenon. The unique signal observed in carbon tetrachloride may come from a fast exchange between bound and free xenon, because a significantly wider signal is observed at 258 K compared to 293 K (data not shown). Because all other tested solvents contain at least one proton, they may reduce the xenon exchange rate by the partial entry of that proton. This does not occur for carbon tetrachloride.

Cryptophanes **2**, **7**, **8**, **9, 10**, and **11** differ only by the nature of the substituents $R_1$ and $R_2$ on the aromatic rings. The chemical shifts of xenon in **2**, **8**, **9**, and **10** are very similar at room temperature. In this series, Xe@**7** is the most upfield shifted. Because calculations indicate that xenon is deshielded when it approaches closely a host atom,[35] it seems that the deshielding effect is more important when an alkoxy group is in position $R_1$ or $R_2$, as in **2**, **8**, **9**, and **10**, than when it is replaced by a proton, as in **7**. Cryptophane **11** has an intermediate situation in which only half the aromatic rings carry an alkoxy group, inducing an average value of the xenon chemical shift between those of **7** and **2**. However, the exact formula of the alkoxy group seems to only slightly influence xenon shielding, because the xenon frequency bandwidth is very narrow (between 66.0 and 67.2 ppm) for **2**, **8**, **9**, and **10**. These results can be compared to those obtained by Pines et al. on derivatives of cryptophane **2** bearing one bulky biotinylated substituent.[9,39,40] In these cases,

and especially when the substituent is bound to avidin, the signal of caged xenon is shifted downfield by several ppm. This seems to come from a cage distortion.[35] This is not observed when the cryptophane moiety bears smaller substituents such as those of **8**, **9**, and **10**, perhaps because *O*-benzyl and butoxy substituents are not bulky enough to significantly modify the cage conformation.

**Evolution of Xenon Chemical Shift with Temperature.** The chemical shift of xenon encapsulated by each of the cryptophanes **1**−**12** is downfield shifted with temperature. The slopes of the caged xenon chemical shift as a function of temperature are reported in Figure 3 and can be sorted into four groups:

- Xe@**10**: 84 ppb $K^{-1}$
- Xe@**1**, Xe@**8**, Xe@**9**: approximately 150 ppb $K^{-1}$
- Xe@**2**, Xe@**3**, Xe@**4**, Xe@**6**, Xe@**11**, Xe@**12**: approximately 225 ppb $K^{-1}$
- Xe@**5**, Xe@**7**: approximately 300 ppb $K^{-1}$

The temperature-dependent behavior of the xenon chemical shift can be interpreted as xenon exploring regions not easily accessible at lower temperature, as a consequence of the deformation of the xenon electron cloud and increased conformational flexibility of the cage as temperature increases.[35] The importance of these effects varies among the different cryptophanes. Cryptophane **5** bears the same substituents on the aromatic rings as cryptophanes **2**, **3**, **4**, and **6** but exhibits a significantly higher chemical-shift variation. Because the calculated cavity volume of **5** is slightly smaller than those of **4** and **6** (Table 2), the xenon mobility in the cavity of **5** may be close to that in the latter two and therefore cannot explain the observed effect. The temperature dependence of the xenon chemical shift in **5** may be due instead to the relatively low energy barriers that the butanedioxy linker has to cross in order to adopt twisted conformations that tend to minimize the size of the cavity or extended conformations that maximize it.

It appears that, for cryptophanes with ethanedioxy linkers, the slope decreases if bulky moieties are attached to the aromatic rings, as can be observed by comparing cryptophane **7** (no aromatic substituents), **11** or **2** (methoxy groups), and **8** or **9** (benzyloxy groups). This may be interpreted as an increase in the energy barrier to cage distortion when bulkier groups are present, thus making high-energy conformations less accessible. Moreover, Figure 3 shows that the number of aromatic ring substituents does not significantly affect the slope as shown by comparison of cryptophanes **8** and **9** or cryptophanes **2** and **11**.

Cryptophane **10** exhibits by far the lowest temperature-dependent variation of the series, which can be interpreted as due to the presence of flexible butyl groups that hinder the access of solvent molecules to bound xenon. Moreover, van der Waals interaction between butoxy groups may reduce the cage's conformational freedom.

The difference in the xenon temperature coefficient slopes observed for **11** and **12**, which differ by the connectivity of their linkers (syn- and anticryptophanes), cannot easily be explained without the help of the calculation of the potential energy surface, particularly with regard to the relative position of the two cyclotriveratrylene units.

The experimental slope for Xe@**1** is significantly lower than that of Xe@**7**. Because of a much smaller volume available for encapsulated xenon in **1** than in **7**, the noble gas may interact with all atoms that constitute the cavity of **1** simultaneously, a situation that does not occur for **7**. Also, **1** is more rigid than **7**, particularly when filled with xenon. Finally, because of the large portals of **7**, the influence of the solvent could accentuate the Xe@**7** chemical-shift variation.

**Release Rate of Bound Xenon.** The in−out exchange rate of xenon is an important parameter for biosensing applications. It has to be slow on the xenon chemical-shift time scale in order to enable observation of a specific signal for caged xenon and furthermore to give rise to a sharp signal. But the release rate must also be high enough to allow the replenishment of cryptophane cages with polarized xenon between acquisitions.[39,41,42] Previous work evidenced the importance of the nature of the tether linking the cryptophane moiety to the recognition antenna on the caged xenon line width.[40] One of the aims of the present study is to examine the effect of various cryptophane cores and their substituents on the xenon in−out exchange rates.

In the present study, the xenon release rate is estimated from the line width of the encapsulated noble gas signal (see Materials and Methods). Although this measurement is not precise, most of the spurious effects are canceled by recording spectra at different temperatures. For instance, the magnetic-field inhomogeneity contribution to the line width has been estimated from experiments at the lowest temperature examined, where exchange is the slowest. Furthermore, the xenon release rates are used only in a comparative way by using mixtures of cryptophanes. This method ensures that both temperature and xenon concentration, parameters that greatly affect the kinetics, are the same along a series.

The influence of the cage stereoisomerism on xenon in−out kinetics has been assessed through the study of a mixture of cryptophanes **11** and **12**. $^{129}$Xe NMR spectra under conditions of a large excess of thermally polarized xenon indicate that the release rate is much faster for **12** than for **11** (data not shown). Portal sizes were found to be similar in the crystallographic structures of **11** and **12**.[6] However, when the cages contain a xenon atom, the aromatic protons in $R_1$ positions, according to Scheme 1, are deshielded by 0.6 ppm in **12** compared to those of **11**.[43] This suggests that both cryptophanes explore significantly different conformational spaces, inducing different global xenon release rates.

It appears that the presence of the methoxy groups sterically hinders the release of xenon. For example, the rate is about one order of magnitude higher for **7** than for **2**, as observed in the $^{129}$Xe spectrum of a mixture of both cryptophanes (Figure S4 in the Supporting Information). This observation is supported by a slightly higher release rate of xenon for **11** than for **2**, at least for temperatures above 265 K (Figure S5 in the Supporting Information). At these low temperatures, the small kinetic difference can be interpreted as one methoxy group per portal being sufficient to hinder the release of xenon. At higher temperature, the cryptophane can attain conformations where a single methoxy group is less able to hinder the passage of xenon. The presence of a second methoxy group close to each portal, as in **2**, may further slow down the release of the noble gas.

The $^{129}$Xe spectra of a mixture of cryptophanes **2, 3, 4, 6** enable a comparison of the xenon release rates (Figure 4). At higher pressure, similar line widths are observed for Xe@**2**, Xe@**3**, Xe@**4**, and Xe@**6**. This may be explained in part by lower magnetic-field homogeneity due to a macroscopic effect of susceptibility variation caused by xenon bubbles.

At lower noble-gas pressure, the line widths reveal the intrinsic cryptophane−xenon dissociation rates. The line widths, decreasing from Xe@**2** to Xe@**6,** indicate that xenon exchange is faster for the smaller cavities than for the larger ones. This behavior, opposite to that observed for the series of water-soluble cryptophane congeners, where the rates increased along the series, appears surprising.[41] By considering that the van der

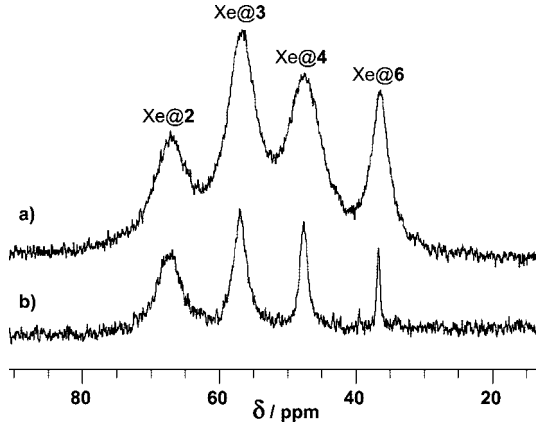


**Figure 4.** High-field region of the laser-polarized $^{129}$Xe NMR spectrum of a mixture of **2, 3, 4, 6** at concentrations of 1.8, 3.0, 6.4, and 10.7 mM, respectively, under a xenon pressure of (a) $1.6 \times 10^5$ Pa and (b) $3.10^4$ Pa, at $T = 295$ K (one scan). A 10 Hz Lorentzian apodization has been applied on the FID before Fourier transformation.

Waals diameter of chlorine is comparable to the portal size in **6**, a possible explanation is that solvent molecules partially penetrate the cavity, thereby slowing down the xenon in−out exchange rate. As the size of the portals progressively decreases in the order **6**, **4**, **3**, **2**, the blocking interaction of the solvent with the portal is limited.[44] At higher pressure however, the replacement of a xenon atom in the cavity by another xenon atom appears more efficient for the largest cryptophane, **6**. Another explanation could be a folding of the structure of **6** at low xenon pressure, giving rise to a slow xenon exchange through a concerted process involving deformation of the cage and encapsulation of xenon.

Finally, the recent synthesis of **1** provides a cage molecule with much lower xenon release rate: 2.4 Hz at 293 K,[2] about 2 orders of magnitude lower than for **2**. The in−out exchange of xenon is drastically reduced in **1** because the average size of the portals is smaller than the diameter of xenon and because the host appears rather rigid. That exchange is still possible, maybe because of the distortion of the xenon electronic cloud. Indeed, recent work supports this assumption, because a chloromethane molecule possessing a similar van der Waals volume as xenon but a lower polarizability does not enter the cavity of **1** under the same experimental conditions. This result will be reported in due course.

**Xenon Longitudinal Relaxation.** The longitudinal relaxation time values, $T_1$, measured on signals characteristic of xenon free in solution and encapsulated in cryptophanes are always similar, within the experimental error. This comes from a fast xenon exchange (faster than 10 Hz) on the relaxation time scale. The averaged xenon $T_1$ is expressed as:

$$\frac{1}{T_1} = \frac{1}{T_1^{\text{caged}}} x_{\text{caged}} + \frac{1}{T_1^{\text{free}}}(1 - x_{\text{caged}}) \qquad (3)$$

where $x_{\text{caged}}$ is the fraction of caged xenon.

Because the relaxation time of the xenon free in solution is very long, on the order of several minutes, the $T_1^{\text{caged}}$ value of encapsulated xenon may be extracted directly from the experimental $T_1$ and the relative xenon populations in both environments, measured by the area of the corresponding signals. The $T_1^{\text{caged}}$ values of xenon in five cryptophanes, **1**, **2**, **7**, **8**, and **11**, at 293 K, are given in Table 3. The choice of the method only slightly influences the extracted $T_1$ value. The value obtained for **2** is slightly higher than the value of 16.4 s estimated by Luhmer et al.[29] but remains within the experimental error.

**TABLE 3: Longitudinal Relaxation Times of Encapsulated Xenon at 293 K**

| Cryptophane | 1 | 2 | 7 | 8 | 11 |
|---|---|---|---|---|---|
| $T_1^{\text{caged}}$ (s) | $15.1 \pm 2.4^a$<br>$12.1 \pm 0.7^b$ | $19.1 \pm 4.7^b$ | $3.9 \pm 0.5^a$ | $9.3 \pm 1.1^a$ | $5.7 \pm 0.3^a$ |

[a] Method using peak area monitoring. [b] Inversion−recovery method.

The $T_1$ decrease in the **2**, **11**, **7** series, along which the number of methoxy substituents decreases, can be interpreted as due to a more efficient relaxation of the noble gas with the aromatic ring protons than with the more distant and mobile methoxy groups. For **1** and **7**, which differ by the length of the three linkers, it appears that the $T_1$ value of xenon bound to the former is significantly higher than in the latter, partly because each linker bears only two protons instead of four. Moreover, the two protons of the O−$CH_2$−O linker point away from the cavity and are therefore more distant from the encapsulated xenon atom. The $T_1$ value of xenon in **1** where alkoxy linkers are deuterated has been measured to be $12.8 \pm 1.5$ s. This value is only slightly higher than that of the fully protonated form of **1**. As for the chemical shifts, this is in agreement with a conformation of O−$CH_2$−O linkers where hydrogen atoms point outward the cavity. These experimental results may also be compared with those obtain with a water-soluble cryptophane derivative of **2**, where $T_1^{\text{caged}}$ significantly depends on the deuteration level of the alkoxy linkers and acetate substituents and where the encapsulated xenon chemical shift differs by ca. 1 ppm between both isotopomers.[41]

The two trends observed for **1**, **2**, and **7** suggest that a cryptophane molecule having short linkers such as those in **1** and bearing methoxy groups such as in **2** would result in an even longer $T_1$ and thus lead to better conservation of the out-of-equilibrium xenon polarization. Obviously, this analysis only considers structural aspects of the Xe@cryptophane complexes. Undoubtedly, the dynamics of the complexes also have a large influence through the rotational correlation time of the encapsulated noble gas. The difference of longitudinal relaxation time for xenon encapsulated in **7** and in **8** evidences that the aromatic protons contribute greatly to the relaxation of the encapsulated xenon. Their replacement by benzyloxy groups on three of the six aromatic rings is sufficient to lengthen the relaxation time by a factor 2.4.

## Conclusion

The analysis of a family of 12 cryptophanes shows that their interaction with xenon involves a high variability of NMR parameters. In order to rationally design biosensors for specific applications based on $^{129}$Xe NMR, several trends related to their physical behavior can be drawn from this work. As expected, the affinity of the host for xenon strongly depends on the quality of the match between the cavity size and the diameter of the noble gas atom. The smallest cryptophane exhibits the highest binding constant with xenon, at the price however of slower in−out xenon exchange less adequate for the $^{129}$Xe-NMR-based biosensing approach. The exchange rate is an important parameter for this application, because it will govern the capability to reload the cage with laser-polarized xenon after each radio frequency excitation.[45] The cavities of cryptophanes delimited by portals of a size similar to that of solvent molecules enable a wide range of in−out exchange rates to be spanned. We have emphasized the fact that size is not the sole parameter that acts on the exchange rate; flexible hydrophobic substituents

can seriously slow down the exchange, as in the case of **10**. Moreover, the exchange rate is significantly increased in the syn-isomer cryptophane compared to the anti-isomer, as exemplified by **11** and **12**.

The longitudinal self-relaxation time of encapsulated xenon is also a key parameter, because it influences the sensitivity of the NMR experiments. It is observed that cryptophanes bearing the shortest alkoxy linkers and the most substituted aromatic rings induce the slowest xenon relaxation because of the smaller number of protons in close proximity to the encapsulated noble gas. Indeed, it was shown previously that for some water soluble cryptophanes, deuteration of the aromatic ring proton sites also acts significantly on xenon $T_1$.[41] Obviously, our study, performed in halogenated solvents, cannot fully prefigure the xenon properties experienced in water, but it gives trends to aid in the conception of new cage molecules adapted to the environment of in vivo experiments around 310 K.

The effect of the solvent has been suggested not only for the in−out exchange rate but also for the resonance frequency of caged xenon. In aqueous solvents, it is nevertheless expected that the water molecules will have a smaller effect on the chemical shifts. However, when modifying the size of the cage, its stereochemistry, or to a lesser extent the substituents on the aromatic rings, will give rise to specific spectral signatures of the new hosts, enabling multiplexing applications.

From our study, it is interesting to note that cryptophanes **1** and **6** (i.e., the smallest and the biggest host molecules) show some resemblance when dealing with the interaction with xenon. In 1,1,2,2-tetrachloroethane, the chemical shifts of caged xenon are the most upfield shifted among those of the 12 cryptophanes. Also, the line widths of these signals are the sharpest at low xenon concentration, indicating a very slow exchange. This could indicate that thanks to the flexibility of the alkyldioxy chains of **6**, this host exists under a folded form, with a small cavity offered to xenon. Such an adaptation effect may occur as soon as the linker length has three carbon atoms, as evidenced by the line widths observed on the $^{129}$Xe spectrum of **2**, **3**, **4**, **6** at low xenon concentration.

**Acknowledgment.** Financial support from the French Ministry of Research (ANR Program Physico-Chimie du Vivant 2006) is greatly acknowledged. H.F. is grateful for financial support from a U.S. National Science Foundation International Research Fellowship grant (no. 0502393).

**Supporting Information Available:** This material is available free of charge via the Internet at http://pubs.acs.org.

## References and Notes

(1) Canceill, J.; Lacombe, L.; Collet, A. *J. Am. Chem. Soc.* **1985**, *107*, 6993.
(2) Fogarty, H. A.; Berthault, P.; Brotin, T.; Huber, G.; Desvaux, H.; Dutasta, J.-P. *J. Am. Chem. Soc.* **2007**, *129*, 10332.
(3) Gabard, J.; Collet, A. *J. Chem. Soc., Chem. Commun.* **1981**, 1137.
(4) Brotin, T.; Dutasta, J.-P. *Eur. J. Org. Chem.* **2003**, 973.
(5) Canceill, J.; Lacombe, L.; Collet, A. *J. Am. Chem. Soc.* **1986**, *108*, 4230.
(6) Canceill, J.; Cesario, M.; Collet, A.; Guilhem, J.; Riche, C.; Pascard, C. *J. Chem. Soc., Chem. Commun.* **1986**, 339.
(7) Roy, V.; Brotin, T.; Dutasta, J.-P.; Charles, M.-H.; Delair, T.; Mallet, F.; Huber, G.; Desvaux, H.; Boulard, Y.; Berthault, P. *ChemPhysChem* **2007**, *8*, 2082.
(8) Hilty, C.; Lowery, T. J.; Wemmer, D. E.; Pines, A. *Angew. Chem. Int. Ed.* **2006**, *45*, 70.
(9) Spence, M. M.; Rubin, S. M.; Dimitrov, I. E.; Ruiz, E. J.; Wemmer, D. E.; Pines, A.; Qin Yao, S.; Tian, F.; Schultz, P. G. *Proc. Natl. Acad. Sci. U.S.A.* **2001**, *98*, 10654.
(10) Brotin, T.; Devic, T.; Lesage, A.; Emsley, L.; Collet, A. *Chem. Eur. J.* **2001**, *7*, 1561.
(11) Brotin, T.; Roy, V.; Dutasta, J.-P. *J. Org. Chem.* **2005**, *70*, 6187.
(12) Cavagnat, D.; Buffeteau, T.; Brotin, T. *J. Org. Chem.* **2008**, *73*, 66.
(13) Canceill, J.; Collet, A. *J. Chem. Soc., Chem. Commun.* **1983**, 1145.
(14) Canceill, J.; Collet, A.; Gottarelli, G. *J. Am. Chem. Soc.* **1984**, *106*, 5997.
(15) Vedejs, E.; Fuchs, P. L. *J. Am. Chem. Soc.* **1973**, *95*, 822.
(16) Herman, R. M. *Phys. Rev.* **1965**, *137A*, 1062.
(17) Walker, T. G.; Happer, W. *Rev. Mod. Phys.* **1997**, *69*, 629.
(18) Desvaux, H.; Gautier, T.; Le Goff, G.; Pétro, M.; Berthault, P. *Eur. Phys. J. D* **2000**, *12*, 289.
(19) Bartik, K.; Luhmer, M.; Dutasta, J.-P.; Collet, A.; Reisse, J. *J. Am. Chem. Soc.* **1998**, *120*, 784.
(20) Segebarth, N.; Aïtjeddig, L.; Locci, E.; Bartik, K.; Luhmer, M. *J. Phys. Chem. A* **2006**, *110*, 10770.
(21) Pollack, G. L.; Himm, J. F. *J. Chem. Phys.* **1982**, *77*, 3221.
(22) Pollack, G. L.; Himm, J. F.; Enyeart, J. *J. Chem. Phys.* **1984**, *81*, 3239.
(23) Pollack, G. L.; Kennan, R. P.; Himm, J. F. *J. Chem. Phys.* **1989**, *90*, 6569.
(24) Kennan, R. P.; Pollack, G. L. *J. Chem. Phys.* **1988**, *89*, 517.
(25) Clever, H. L. *IUPAC solubility data series*; Pergamon Press: Oxford, 1979.
(26) Al-Hayan, M. N. M. *J. Chem. Thermodyn.* **2006**, *38*, 427.
(27) Rogers, M.; Woodbrey, J. *J. Phys. Chem.* **1962**, *66*, 540.
(28) Miller, K. W.; Reo, N. V.; Schoot Uiterkamp, J. M.; Stengle, D. P.; Stengle, T. R.; Williamson, K. L. *Proc. Natl. Acad. Sci. U.S.A.* **1981**, *78*, 4946.
(29) Luhmer, M.; Goodson, B. M.; Song, Y.-Q.; Laws, D. D.; Kaiser, L.; Cyrier, M. C.; Pines, A. *J. Am. Chem. Soc.* **1999**, *121*, 3502.
(30) Bartik, K.; Luhmer, M.; Heyes, S. J.; Ottinger, R.; Reisse, J. *J. Magn. Reson. B* **1995**, *109*, 164.
(31) El Haouaj, M.; Luhmer, M.; Ho Ko, Y.; Kim, K.; Bartik, K. *J. Chem. Soc., Perkin Trans. 2* **2001**, 804.
(32) Kim, B. S.; Ko, Y. H.; Kim, Y.; Lee, H. J.; Selvapalam, N.; Lee, H. C.; Kim, K. *Chem. Commun.* **2008**, 2756.
(33) Desvaux, H.; Huber, J. G.; Brotin, T.; Dutasta, J.-P.; Berthault, P. *ChemPhysChem* **2003**, *4*, 384.
(34) Mecozzi, S.; Rebek, J., Jr. *Chem. Eur. J.* **1998**, *4*, 1016.
(35) Sears, D. N.; Jameson, C. J. *J. Chem. Phys.* **2003**, *119*, 12231.
(36) Straka, M.; Lantto, P.; Vaara, J. *J. Phys. Chem. A* **2008**, *112*, 2658.
(37) Xe@**5**, the signal of which is strongly low-field shifted, cannot be incorporated in the previous series. We are unable to explain such an effect.
(38) Canceill, J.; Lacombe, L.; Collet, A. *J. Chem. Soc., Chem. Commun.* **1987**, 219.
(39) Spence, M. M.; Ruiz, E. J.; Rubin, S. M.; Lowery, T. J.; Winssinger, N.; Schultz, P. G.; Wemmer, D. E.; Pines, A. *J. Am. Chem. Soc.* **2004**, *126*, 15287.
(40) Lowery, T. J.; Garcia, S.; Chavez, L.; Ruiz, E. J.; Wu, T.; Brotin, T.; Dutasta, J.-P.; King, D. S.; Schultz, P. G.; Pines, A.; Wemmer, D. E. *ChemBioChem* **2006**, *7*, 65.
(41) Huber, G.; Brotin, T.; Dubois, L.; Desvaux, H.; Dutasta, J.-P.; Berthault, P. *J. Am. Chem. Soc.* **2006**, *128*, 6239.
(42) Schröder, L.; Lowery, T. J.; Hilty, C.; Wemmer, D. E.; Pines, A. *Science* **2006**, *314*, 446.
(43) Canceill, J.; Lacombe, A.; Collet, A. C. R. *Acad. Sci. Paris Ser. II* **1984**, *298*, 39.
(44) For water-soluble cryptophanes, the water molecule, contrary to 1,1,2,2-tetrachloroethane-$d_2$, is small enough to enter the cavity of all members of the series.
(45) Schröder, L.; Chavez, L.; Meldrum, T.; Smith, M.; Lowery, T. J.; Wemmer, D. E.; Pines, A. *Angew. Chem. Int. Ed.* **2008**, *47*, 4316.

JP807425T